Theory and Measurement of the X-Ray Satellite Reflections in Holmium Due to the Aspherical 4f Charge Density*

D. T. KEATING
Brookhaven National Laboratory, Upton, New York 11973
(Received 11 July 1968)

The theory and experimental measurement of the satellite reflections appearing about the normal Laue-Bragg reflections in holmium are discussed. These reflections arise from the asphericity of the 4f charge density as distinct from the core charge density. In holmium metal the $5d^1$ and $6s^2$ valence electrons are believed to enter the conduction bands, leaving a tripositive ion core approximated by the configuration $^5I_8$. The 4f shell lacking four electrons is screened from the crystalline environment by the filled $5s^2$ and $5p^6$ shells. Because of the unpaired electrons in the 4f shell, the ions have a magnetic moment which between 20 and 132°K tends to align them in a flat spiral with a propagation vector τ lying along the hexagonal axis of the crystal. This tendency of the ions to order into such a spiral, coupled with the aspherical charge density, induces periodicities in the scattering of the structure containing the first three even harmonics of τ. These periodicities produce x-ray satellite reflections about all allowed reflections except $(00\bar{0}\cdot L)$ at ± 2, ± 4, and $\pm 6\tau$. At a nonzero temperature the ions are disordered to the extent that they are distributed amongst states with magnetic quantum number M and inner quantum number $J=8$. Using the molecular-field approximation suggested by Nagamiya to describe this disorder, it was found that past observation of neutron satellite intensities of Koehler *et al.* were explained. The theory was then used to calculate the average x-ray scattering factor from the scattering factors for the various ionic states M whose computation rests upon parameters derived by Blume *et al.* from recently determined Hartree-Fock wave functions. The agreement with experimentally observed values of the scattering of the first satellite pair about the $(22\bar{4}\cdot 0)$ reflection discussed in the paper is excellent.

INTRODUCTION

THE theory and experimental measurement of the satellite reflections appearing about the normal Laue-Bragg reflections in holmium are discussed. These reflections arise from the asphericity of the 4f charge density as distinct from the core charge density. Holmium is a rare-earth metal, the 4f shell lacking four electrons of being filled. The $6s^2$ and $5d^1$ electrons are believed to enter the conduction band leaving a tripositive ion core. However, the 4f shell is deeply embedded in the ion's interior[1] and is screened from the crystalline environment by the filled $5s^2$ and $5p^6$ shells so that the configuration of the ion core is approximately described[2] by the spectroscopic state $^5I_8$. Because of the unpaired electrons in the 4f shell, a magnetic moment results. Measurements of the magnetic susceptibility of holmium in the paramagnetic region give values for the total effective magnetic moment of $10.6\mu_B$ [3] to $10.9\mu_B$,[4,5] while measurements of the saturation magnetization give values between $10.0\mu_B$ [6] and $10.34\mu_B$.[5] These values are in good agreement with the values $g[J(J+1)]^{1/2}=10.6\mu_B$ for total effective magnetic moment and $gJ=10.0\mu_B$ for the component of the magnetic moment along the **z** axis of the ion for the spectroscopic state $^5I_8$. J is the inner quantum number equal to 8, and g is the gyromagnetic ratio given by the Landé formula

$$g=1+\frac{J(J+1)-L(L+1)+S(S+1)}{2J(J+1)}=\frac{5}{4}$$

for $L=6$ and $S=2$ for the spectroscopic state $^5I_8$.

Holmium has a hexagonal close-packed structure and the magnetic moment is found in three magnetic phases.[7] Above the Néel temperature of 131.4°K the structure is paramagnetic with the magnetic moments oriented at random. Between the Néel temperature and the Curie point of 19.4°K, it is antiferromagnetic with the average moment aligned in the basal planes of the structure, but, as one proceeds from one basal plane to the next, the direction of the average moment rotates. This angle of rotation varies from nearly 51° per layer at the Néel point to precisely 30° per layer at the Curie point. The configuration is that of a flat spiral with a propagation vector τ normal to the basal planes of magnitude equal to the reciprocal of the wavelength of the spiral. Below the Curie point the structure is ferromagnetic with a conical spiral having a moment of $1.7\mu_B$ perpendicular to the basal planes and a component $9.7\mu_B$ in the basal planes. The turn angle remains fixed at 30° per layer. Koehler *et al.*[8,9] have reported a tendency for the moments in the basal plane to bunch preferentially around the easy directions of magnetization at 4.2°K. However, this paper is

* Work performed under the auspices of the U. S. Atomic Energy Commission.

[1] A. J. Freeman and R. E. Watson, Phys. Rev. **127**, 2058 (1962).
[2] B. G. Wybourne, *Spectroscopic Properties of Rare Earths* (John Wiley & Sons, Inc., New York, 1965), p. 3.
[3] H. Bommer, Z. Anorg. Allgem. Chem. **242**, 277 (1939).
[4] B. L. Rhodes, S. Legvold, and F. H. Spedding, Phys. Rev. **109**, 1547 (1958).
[5] D. L. Strandburg, S. Legvold, and F. H. Spedding, Phys. Rev. **127**, 2046 (1962).
[6] W. E. Henry, in *Rare-Earth Research*, edited by Le Roy Eyring (Gordon and Breach, Science Publishers, Inc., New York, 1965). p. 45.
[7] W. C. Koehler, J. Appl. Phys. **36**, 1078 (1965).
[8] W. C. Koehler, J. W. Cable, M. K. Wilkinson, and E. O. Wollan, Phys. Rev. **151**, 414 (1966).
[9] W. C. Koehler, J. W. Cable, H. R. Child, M. K. Wilkinson, and E. O. Wollan, Phys. Rev. **158**, 450 (1967).

devoted entirely to the diffraction phenomena observed from holmium in the antiferromagnetic state, with primary emphasis on the position and intensity of the x-ray satellites. Nevertheless, the variation of the intensity of the neutron satellites with temperature is given a theoretical explanation because of its relevance in confirming the theory necessary for explaining the x-ray satellite intensities.

Koehler[7] observed neutron satellites from a single crystal of holmium and has given the explanation for their production and position in the neutron case.[10] Because the magnetic scattering amplitude is a vector quantity related to the magnitude and direction of the ion's magnetic moment, the rotation of the mean moment in the holmium structure introduces an additional periodicity in the structure, in this case not commensurate with the lattice periodicity. This additional periodicity, that of the spiral, produces neutron satellites at $\pm\tau$ about all allowed nuclear reflections. It was first suggested by Blume[11] that because of the aspherical charge density's orientation relative to the ion's magnetic moment, there should be an additional periodicity in the x-ray structure as well, and that x-ray satellites analogous to the neutron satellites should be observable.

Preliminary calculations assuming a fully ordered antiferromagnetic state and a single determinantal wave function for the ion with the $4f$ shell filled according to Hund's rule predicted three x-ray satellites about all reflections except $(00\bar{0}\cdot L)$ at the distances ± 2, ± 4, and $\pm 6\tau$. However, the predicted integrated reflections were all exceedingly small, $\sim 10^{-10}$ even for the most favorable satellite pair about the $(22\bar{4}\cdot 0)$ reflection, indicating stringent experimental conditions for their detection. Experimental observation of the satellites at 77.4 and 27.3°K at their expected positions confirmed their existence. However, their intensities were found to be considerably less than the preliminary estimates. In an attempt to rationalize this discrepancy the effect of magnetic ordering using the molecular field theory of helical spin configurations as suggested by Nagamiya[12] was considered. In this theory the mean magnetic moment is given by the Brillouin function whose argument involves the mean moment and the ratio of the Néel temperature and temperature. The mean moment as a function of temperature was found by the solution of this equation. The neutron scattering amplitude is directly proportional to this mean moment and the scattering factor observed by Koehler *et al.*[8] is in excellent agreement (see Fig. 3) with this solution. Since the molecular field theory was in such good agreement with these neutron results, it was decided to adapt the theory to the evaluation of the x-ray scattering factor. In this case this amounted to finding the wave functions for all states M of the ${}^5I$ multiplet with $J=8$, computing the scattering factor for each state M, and then weighting the scattering factor for each state M by the Boltzmann factor appropriate for the state. These scattering-factor calculations ultimately rest on the nonrelativistic Hartree-Fock wave functions including exchange determined by Freeman and Watson[1] for a large number of tripositive rare-earth ions. However, Blume, Freeman, and Watson[13] have tabulated all the radial integrals and other form-factor data from these wave functions, and the data for Ho^{3+} was interpolated between Dy^{3+} and Er^{3+} from their tables. The final theoretical intensity for the x-ray satellites is in good agreement with experiment. The theory predicting the position and intensity of the x-ray satellites is developed and measurement of the satellites is described.

THEORY

We can think about the problem of the production of x-ray satellites as a three-part problem. The first part involves the determination of the scattering of x radiation by an ion with a nonspherical charge density and characterized by the inner quantum number J and the magnetic quantum number M as the angle between the ionic $\mathbf{z}$ axis and $\boldsymbol{\kappa}$ is varied. Here $\boldsymbol{\kappa}$ is the difference between the incoming and scattered wave vectors. The second part of the problem consists in determining the interference effects from the structure when the ion is quantized such that the direction of the $\mathbf{z}$ axis, and hence the scattering, varies periodically throughout the structure with the turn angle described by the propagation vector $\boldsymbol{\tau}$. Finally, we must take into account that as the temperature is raised the number of states M that can be occupied increases and the scattering from each of these M states must be weighted by the appropriate Boltzmann factor to find the correct coherent scattering from the structure at a given temperature above absolute zero.

If the wave function of an ion is represented by an antisymmetric combination of N one-electron spin orbitals such as

$$\psi(r_1 r_2 \cdots r_n) = N^{-1/2} \begin{vmatrix} \mu_1(r_1)\mu_1(r_2)\cdots\mu_1(r_n) \\ \mu_2(r_1)\mu_2(r_2)\cdots\mu_2(r_n) \\ \cdots \\ \mu_n(r_1)\mu_n(r_2)\cdots\mu_n(r_n) \end{vmatrix}, \quad (1)$$

the approximate form of the coherent scattering from an ion with such a representation is[14]

$$f_{\text{ion}} = \sum_{nlm_l m_s} (\mu_{nlm_l m_s}(r) | e^{i\kappa\cdot r} | \mu^*_{nlm_l m_s}(r)) = \sum_{nlm_l m_s} f_{nlm_l m_s}(\kappa), \quad (2)$$

[10] W. C. Koehler, Acta Cryst. **14**, 535 (1961).
[11] M. Blume (private communication).
[12] T. Nagamiya, in *Solid State Physics*, edited by F. Seitz and D. Turnbull (Academic Press Inc., New York, 1967), Vol. 20, p. 305.
[13] M. Blume, A. J. Freeman, and R. E. Watson, J. Chem. Phys. **37**, 1245 (1962).
[14] R. W. James, *The Optical Principals of the Diffraction of X rays* (G. Bell and Sons, Ltd., London, 1958), Chap. 3.

where the $f_{nlm_lm_s}(\kappa)$ are the diagonal matrix components of $e^{i\kappa\cdot r}$ with respect to the one-electron spin orbitals $\mu_{nlm_lm_s}(r)$ in Eq. (1). If linear combinations of functions such as in Eq. (1) are used to obtain a better representation of the ion, then the coherent scattering from this representation will be the sum of the scattering from each term as in Eq. (2) weighted by the magnitudes squared of the coefficients used in the representation, or the occupation numbers. The coherent scattering from the crystal will appear then as if the ions in the structure were actually distributed amongst the stationary states used in the representation. If we let $\Gamma_{nlm_lm_s}{}^2(M)$ be the sum of the occupation numbers of all the determinantal wave functions containing the one-electron spin orbital $\mu_{nlm_lm_s}(r)$ in the representation M, we can write the scattering factor as

$$f_{\text{ion}}=\sum_{nlm_lm_s}\Gamma_{nlm_lm_s}{}^2(M)f_{nlm_lm_s}(\kappa). \tag{3}$$

The sum in Eq. (3) is over all the one-electron spin orbitals used in the representation. Since the determinantal wave functions that we will be dealing with differ only in the $4f$ spin orbitals the Γ's will be unity for all spin orbitals other than those of the $4f$ shell.

Freeman and Watson[1] have recently obtained "conventional" Hartree-Fock wave functions for the rare-earth ions. In the conventional treatment the one-electron spin orbitals are assumed to be separable into products of radial functions $R_{nl}(r)$, spherical harmonics[15] $Y_{lm}(\theta,\phi)$, and spin functions with only one $R_{nl}(r)$ per shell, i.e., the $R_{nl}(r)$ are dependent only on the total quantum number n and the azimuthal quantum number l, and are independent of the magnetic quantum number m_l and spin quantum number m_s. With these assumptions the $f_{nlm_lm_s}(\kappa)$ in Eq. (2) reduce to the evaluation of

$$f_{nlm_lm_s}(\kappa)=\int_0^\infty\int_0^{4\pi}e^{i\kappa\cdot r}|R_{nl}(r)|^2|Y_{lm_l}(\theta,\phi)|^2\times r^2drd\Omega. \tag{4}$$

With the aid of the expansion formula for the imaginary exponential[16]

$$e^{i\kappa\cdot r}=4\pi\sum_{k,q}i^kj_k(\kappa r)Y_{kq}(\hat{r})Y_{kq}{}^*(\hat{\kappa}), \tag{5}$$

Eq. (4) becomes

$$f_{nlm_lm_s}(\kappa)=4\pi\sum_{k,q}i^k\int_0^\infty j_k(\kappa r)|R_{nl}(r)|^2r^2dr\times\int_0^{4\pi}Y_{kq}(\hat{r})Y_{kq}(\hat{\kappa})|Y_{lm_l}(\hat{r})|^2d\Omega_r. \tag{6}$$

In Eqs. (5) and (6), $\hat{r}$ and $\hat{\kappa}$ symbolize the polar angles of $\mathbf{r}$, the electron position vector, and $\boldsymbol{\kappa}$, the diffraction vector. The $j_k(\kappa r)$ are the usual spherical Bessel functions. The angular integrations in Eq. (6) are expedited by expressing $|Y_{lm_l}(\hat{r})|^2$ in terms of linear combinations of spherical harmonics. The coefficients of expansion, or Gaunt's coefficients, are easily expressed in terms of the 3-j symbols[17] such that one can write

$$|Y_{lm_l}(\hat{r})|^2=\frac{(-1)^{m_l}(2l+1)}{(4\pi)^{1/2}}\sum_{l'=0}^{l'=2l}(2l'+1)^{1/2}\times\begin{pmatrix}l & l & l'\\ m_l & -m_l & 0\end{pmatrix}\begin{pmatrix}l & l & l'\\ 0 & 0 & 0\end{pmatrix}Y_{l'0}{}^*(\hat{r}). \tag{7}$$

The second 3-j symbol vanishes unless $2l+l'$ is even, so that with the aid of Eq. (7), Eq. (6) reduces to

$$f_{nlm_lm_s}(\kappa)=(-1)^{m_l}(2l+1)(4\pi)^{1/2}\sum_{L=0}^{L=l}(-1)^L(4L+1)^{1/2}\times\begin{pmatrix}l & l & 2L\\ m_l & -m_l & 0\end{pmatrix}\begin{pmatrix}l & l & 2L\\ 0 & 0 & 0\end{pmatrix}\times\langle j_{2L}(\kappa)\rangle_{nl}Y_{2L0}(\hat{\kappa}), \tag{8}$$

where

$$\langle j_{2L}(\kappa)\rangle_{nl}=\int_0^\infty|R_{nl}(r)|^2j_{2L}(\kappa r)r^2dr. \tag{9}$$

Blume *et al.*,[13] using the recently determined conventional Hartree-Fock wave functions,[1] have tabulated the scattering factors and values of $\langle j_{2L}(\kappa)\rangle_{43}$ for the $4f$ shell for most of the rare-earth ions. Values for Ho^{3+} can be interpolated easily from their values for Dy^{3+} and Er^{3+}. Expressing the spherical harmonics in terms of their argument, $\cos\theta$, where θ is the angle between $\boldsymbol{\kappa}$ and the $\mathbf{z}$ axis of the ion, Eq. (8) can also be written as

$$f_{nlm_lm_s}(\kappa)=\sum_{p=0}^{p=l}\sum_{L=0}^{L=l}A_{m_lLp}\langle j_{2L}(\kappa)\rangle_{nl}\cos^{2p}\theta. \tag{10}$$

The coefficients A_{m_l00} are always unity. Further, they have the property that

$$\sum_{m_l=-l}^{m_l=l}A_{m_lLp}=2l+1\quad(L=0,\,p=0)\qquad=0\quad(L\neq0). \tag{11}$$

These results follow from a theorem due to Unsöld regarding the angular dependence of wave functions, namely, that the square of the magnitudes of all the angular wave functions corresponding to a given l value is a constant $(2l+1)$, independent of orientation.[18]

[15] See, e.g., M. E. Rose, *Elementary Theory of Angular Momentum*, (John Wiley & Sons, Inc., New York, 1957), p. 240.

[16] See, e.g., A. Messiah, *Quantum Mechanics I* (North-Holland Publishing Co., Amsterdam, 1964), p. 359.

[17] M. Rotenberg, R. Bivins, N. Metropolis, and J. K. Wooster, *The 3-j and 6-j Symbols* (Technology Press, Cambridge, Mass., 1959), p. 9.

[18] See, e.g., J. C. Slater, *Quantum Theory of Atomic Spectra* (McGraw-Hill Book Co., New York, 1960), Vol. I, p. 182.

TABLE I. The coefficients A_{m_lLp} used in Eq. (10) for the scattering factors of the one-electron wave functions of the $4f$ shell.

$p=0$

$\lvert m_l\rvert$ \ L	0	1	2	3
0	1	+4/6	+54/88	+500/528
1	1	+3/6	+ 9/88	−375/528
2	1	0	−63/88	+150/528
3	1	−5/6	+27/88	− 25/528

$p=1$

$\lvert m_l\rvert$ \ L	0	1	2	3
0	0	−12/6	−540/88	−10500/528
1	0	− 9/6	− 90/88	+ 7875/528
2	0	0	+630/88	− 3150/528
3	0	+15/6	−270/88	+ 525/528

$p=2$

$\lvert m_l\rvert$ \ L	0	1	2	3
0	0	0	+630/88	+31500/528
1	0	0	+105/88	−23625/528
2	0	0	−735/88	+ 9450/528
3	0	0	+315/88	− 1575/528

$p=3$

$\lvert m_l\rvert$ \ L	0	1	2	3
0	0	0	0	−23100/528
1	0	0	0	+17325/528
2	0	0	0	− 6930/528
3	0	0	0	+ 1155/528

Thus in Eq. (3) for spin orbitals other than those involving the $4f$ shell, $f_{nlm_lm_s}(\kappa)$ can be replaced by $\langle j_0(\kappa)\rangle_{nl}$. The coefficients $A_{m_lL,p}$ for the $4f$ shell are listed in Table I. Equation (11) is a useful check on the coefficients listed in the table.

Restricting ourselves to linear combinations of determinantal wave functions of the ^5I multiplet in which J and M are good quantum numbers, we can write the scattering factor of the ion as

$$f_M=\sum_{nlm_lm_s}\Gamma_{nlm_lm_s}{}^2(M)\langle j_0(\kappa)\rangle_{nl}+\sum_{m_lm_s}\sum_{L=1}^{3}\sum_{p=0}^{3}\Gamma_{43m_lm_s}{}^2(M)A_{m_lLp}\langle j_{2L}(\kappa)\rangle_{43}\times\cos^{2p}\theta. \quad (12)$$

The first sum of $\langle j_0(\kappa)\rangle_{nl}$ is the usual total ion scattering factor $f_{Ho^{3+}}$ without aspherical effects, and the second sum contains the aspherical effects.

We now consider the combination of determinantal functions necessary to describe the ion with a good inner quantum number J and magnetic quantum number M. It turns out that the single determinantal function for $^5I_8$ given by Hund's rule[19] has good quantum numbers $J=8$, $M=8$, $L=6$, $S=2$, $M_L=6$, and $M_S=2$. The determinant is as in Eq. (1) with the last 10 rows containing the one-electron spin orbitals $\mu_{nlm_lm_s}(r)$ with $n=4$, $l=3$, and the values (m_l,m_s) of $(+3,+\frac{1}{2})$, $(+2,+\frac{1}{2})$, $(+1,+\frac{1}{2})$, $(0+\frac{1}{2})$, $(-1,+\frac{1}{2})$, $(-2,+\frac{1}{2})$, $(-3,+\frac{1}{2})$, $(+3,-\frac{1}{2})$, $(+2,-\frac{1}{2})$, and $(+1,-\frac{1}{2})$. The other functions of the ^5I multiplet for other values of M_L and M_S were found by successively operating on this determinantal function with the step down operators $(L_x-iL_y)_{op}$ and $(S_x-iS_y)_{op}$ and successively renormalizing.[20] Then those linear combinations of these resulting linear combinations of determinantal functions for which $M_L+M_S=M$ were made, the coefficients of combination being the Clebsch-Gordan coefficients.[20] The Clebsch-Gordan coefficients produce normalized wave functions with good quantum numbers J and M, and in this case L and S also. As a result of these operations a series of determinantal functions for each value of M was found: for $|M|=8$, 1 function; $|M|=7$, 5; $|M|=6$, 12; $|M|=5$, 21; $|M|=4$, 33; $|M|=3$, 47; $|M|=2$, 59; $|M|=1$, 67, and for $M=0$, a series of 70 determinantal functions. From the coefficients in these series the sum of the occupation numbers $\Gamma_{43m_lm_s}(M)$ were found and are listed in Table II. The steps outlined leading to Table II become tedious and as an expediency a program was written to carry out the procedure on a CDC-6600 computer. An alternative approach to the method of calculation presented in this section exists using the techniques developed by Racah. The reader is referred to the relevant formulas given by Wybourne[2] on p. 165. Equation (12), along with the results of Table II, allows us to infer that those combinations of determinantal functions describing a particular state M of the ion will produce a scattering factor having an angular variation depending only on even powers of $\cos\theta$. In the case of a spiral arrangement of the ions, $\cos\theta$ varies throughout the structure in a periodic way. It is this dependence of the scattering upon $\cos\theta$ which determines the number of x-ray satellite reflections, and is considered next.

The next consideration is that of expressing the angle θ between $\boldsymbol{\kappa}$ and the $\mathbf{z}$ axis of the ion as a function of the position of the ion in the crystal. The approach is similar to Koehler's[10] for neutron scattering by helical spin structures. For a spiral, such as in holmium, we define a coordinate system where the direction of the spiral axis is defined by its propagation vector $\boldsymbol{\tau}$, the angle between $\boldsymbol{\tau}$ and $\boldsymbol{\kappa}$ is c, and the $\mathbf{z}$ axis of the ion rotates around $\boldsymbol{\tau}$ at the constant angle b. The angle between $\boldsymbol{\kappa}$ and $\mathbf{z}$ is, of course, θ. The angle included between the sides b and c of the spherical triangle b, c, θ we call the angle of rotation α_{ij}. The angle of rotation depends on the position of the ith ion in the jth cell of the structure through

$$\alpha_{ij}=2\pi\boldsymbol{\tau}\cdot(\mathbf{r}_i+\mathbf{r}_j)+\psi, \quad (13)$$

where ψ is an arbitrary phase angle. Thus we can write

$$\cos\theta=\cos b\cos c+\sin b\sin c\cos\alpha_{ij}. \quad (14)$$

[19] See Ref. 18, Vol. I, pp. 285 and 304.
[20] See Ref. 18, Vol. II, Chap. 20.

TABLE II. Sum of the occupation numbers, $\Gamma_{43m_l m_s}{}^2(M)$, for the holmium ion in the state with inner quantum number $J=8$ and magnetic quantum number M.

m_s	$\Gamma_{43+3m_s}{}^2(M)$	$\Gamma_{43+2m_s}{}^2(M)$	$\Gamma_{43+1m_s}{}^2(M)$	$\Gamma_{430m_s}{}^2(M)$	$\Gamma_{43-1m_s}{}^2(M)$	$\Gamma_{43-2m_s}{}^2(M)$	$\Gamma_{43-3m_s}{}^2(M)$
				$M=8$			
$+\frac{1}{2}$	1.0000000	1.0000000	1.0000000	1.0000000	1.0000000	1.0000000	1.0000000
$-\frac{1}{2}$	1.0000000	1.0000000	1.0000000	0.0000000	0.0000000	0.0000000	0.0000000
				$M=7$			
$+\frac{1}{2}$	1.0000000	1.0000000	1.0000000	0.9375000	0.9375000	0.9375000	0.9375000
$-\frac{1}{2}$	1.0000000	1.0000000	0.2500000	0.8125000	0.0625000	0.0625000	0.0625000
				$M=6$			
$+\frac{1}{2}$	1.0000000	1.0000000	0.9000000	0.9750000	0.8750000	0.8750000	0.8750000
$-\frac{1}{2}$	1.0000000	0.7500000	0.4000000	0.6750000	0.4250000	0.1250000	0.1250000
				$M=5$			
$+\frac{1}{2}$	1.0000000	0.9464286	0.8714286	0.9303571	0.8767857	0.8125000	0.8125000
$-\frac{1}{2}$	0.9642857	0.5535714	0.6714286	0.4482143	0.6660714	0.2589286	0.1875000
				$M=4$			
$+\frac{1}{2}$	0.9890110	0.8626374	0.8989011	0.8302198	0.8972527	0.7719780	0.7500000
$-\frac{1}{2}$	0.8928571	0.4972527	0.7939560	0.4049451	0.7131868	0.4395604	0.2582418
				$M=3$			
$+\frac{1}{2}$	0.9553571	0.7905220	0.9141483	0.7520604	0.8804945	0.7664835	0.6909341
$-\frac{1}{2}$	0.8028846	0.5556319	0.7616758	0.5254121	0.6469780	0.6126374	0.3447802
				$M=2$			
$+\frac{1}{2}$	0.8924825	0.7576174	0.8700050	0.7411339	0.8074426	0.7887113	0.6426074
$-\frac{1}{2}$	0.7159091	0.6634615	0.6679570	0.6926823	0.5766733	0.7340160	0.4493007
				$M=1$			
$+\frac{1}{2}$	0.8011364	0.7644231	0.7675699	0.7848776	0.7036713	0.8138112	0.6145105
$-\frac{1}{2}$	0.6499126	0.7600524	0.6058566	0.8056818	0.5736014	0.7875874	0.5673077
				$M=0$			
$+\frac{1}{2}$	0.6888112	0.7867133	0.6496503	0.8272727	0.6209790	0.8111888	0.6153846
$-\frac{1}{2}$	0.6153846	0.8111888	0.6209790	0.8272727	0.6496503	0.7867133	0.6888112
				$M=-1$			
$+\frac{1}{2}$	0.5673077	0.7875874	0.5736014	0.8056818	0.6058566	0.7600524	0.6499126
$-\frac{1}{2}$	0.6145105	0.8138112	0.7036713	0.7848776	0.7675699	0.7644231	0.8011364
				$M=-2$			
$+\frac{1}{2}$	0.4493007	0.7340160	0.5766733	0.6926823	0.6679570	0.6634615	0.7159091
$-\frac{1}{2}$	0.6426074	0.7887113	0.8074426	0.7411339	0.8700050	0.7576174	0.8924825
				$M=-3$			
$+\frac{1}{2}$	0.3447802	0.6126374	0.6469780	0.5254121	0.7616758	0.5556319	0.8028846
$-\frac{1}{2}$	0.6909341	0.7664835	0.8804945	0.7520604	0.9141483	0.7905220	0.9553571
				$M=-4$			
$+\frac{1}{2}$	0.2582418	0.4395604	0.7131868	0.4049451	0.7939560	0.4972527	0.8928571
$-\frac{1}{2}$	0.7500000	0.7719780	0.8972527	0.8302198	0.8989011	0.8626374	0.9890110
				$M=-5$			
$+\frac{1}{2}$	0.1875000	0.2589286	0.6660714	0.4482143	0.6714286	0.5535714	0.9642857
$-\frac{1}{2}$	0.8125000	0.8125000	0.8767857	0.9303571	0.8714286	0.9464286	1.0000000
				$M=-6$			
$+\frac{1}{2}$	0.1250000	0.1250000	0.4250000	0.6750000	0.4000000	0.7500000	1.0000000
$-\frac{1}{2}$	0.8750000	0.8750000	0.8750000	0.9750000	0.9000000	1.0000000	1.0000000
				$M=-7$			
$+\frac{1}{2}$	0.0625000	0.0625000	0.0625000	0.8125000	0.2500000	1.0000000	1.0000000
$-\frac{1}{2}$	0.9375000	0.9375000	0.9375000	0.9375000	1.0000000	1.0000000	1.0000000
				$M=-8$			
$+\frac{1}{2}$	0.0000000	0.0000000	0.0000000	0.0000000	1.0000000	1.0000000	1.0000000
$-\frac{1}{2}$	1.0000000	1.0000000	1.0000000	1.0000000	1.0000000	1.0000000	1.0000000

Since we can always write

$$\cos^{2p}\theta = \sum_{q=0}^{q=2p} B_{pq} \cos q\alpha_{ij}, \tag{15}$$

we can write Eq. (12) for the scattering factor of the ion at the site ij:

$$f_M(ij) = f_{Ho^{3+}} + \sum_{m_l m_s} \sum_{L=1}^{3} \sum_{p=0}^{3} \sum_{q=0}^{q=2p} \Gamma_{43m_l m_s}{}^2(M) \times A_{m_l L p} B_{pq} \langle j_{2L}(\kappa)\rangle_{43} \cos q\alpha_{ij}, \tag{16}$$

where the coefficients B_{pq} are tabulated in Table III.

TABLE III. The coefficients B_{pq} used in Eq. (16). $B_{00}=1$ and $B_{0q}=0$.

q \ p	1	2	3
0	$+(\cos b\cos c)^2+\frac{1}{2}(\sin b\sin c)^2$	$+(\cos b\cos c)^4+3(\cos b\cos c)^2(\sin b\sin c)^2+\frac{3}{8}(\sin b\sin c)^4$	$+(\cos b\cos c)^6+\frac{15}{2}(\cos b\cos c)^4(\sin b\sin c)^2+(45/8)(\cos b\cos c)^2(\sin b\sin c)^4+(10/32)(\sin b\sin c)^6$
1	$+2(\cos b\cos c)(\sin b\sin c)$	$+4(\cos b\cos c)^3(\sin b\sin c)+3(\cos b\cos c)(\sin b\sin c)^3$	$6(\cos b\cos c)^5(\sin b\sin c)+15(\cos b\cos c)^3(\sin b\sin c)^3+(30/8)(\cos b\cos c)(\sin b\sin c)^5$
2	$+\frac{1}{2}(\sin b\sin c)^2$	$+3(\cos b\cos c)^2(\sin b\sin c)^2+\frac{1}{2}(\sin b\sin c)^4$	$+\frac{15}{2}(\cos b\cos c)^4(\sin b\sin c)^2+\frac{15}{2}(\cos b\cos c)^2(\sin b\sin c)^4+\frac{15}{32}(\sin b\sin c)^6$
3	0	$+3(\cos b\cos c)(\sin b\sin c)^3$	$+5(\cos b\cos c)^3(\sin b\sin c)^3+(15/8)(\cos b\cos c)(\sin b\sin c)^5$
4	0	$+\frac{1}{8}(\sin b\sin c)^4$	$+(15/8)(\cos b\cos c)^2(\sin b\sin c)^4+6/32(\sin b\sin c)^6$
5	0	0	$+\frac{3}{8}(\cos b\cos c)(\sin b\,\mathrm{cin}c)^5$
6	0	0	$+\frac{1}{32}(\sin b\sin c)^6$

In addition, $B_{00}=1$ and $B_{0q}=0$. If we set

$$\sum_{m_l m_s}\sum_{L=1}^{3}\sum_{p=0}^{3}\Gamma_{43m_lm_s}{}^2(M)A_{m_lL_p}B_{pq}\langle j_{2L}(\kappa)\rangle = f_{M0}\quad(q=0)$$
$$= 2f_{Mq}\quad(q\neq 0), \tag{17}$$

we may write the scattering factor in Eq. (16) as

$$f_M(ij)=\sum_{q=-6}^{q=+6}[f_{Mq}+\delta(q)f_{\mathrm{Ho}^{3+}}]\times\exp[2\pi iq\boldsymbol{\tau}\cdot(\mathbf{r}_i+\mathbf{r}_j)+iq\psi]. \tag{18}$$

If all the ions are in the state M, the amplitude of the coherent scattering E from a holmium crystal is

$$E=\mathcal{E}\sum_{ij}\sum_{q=-6}^{q=6}(f_{Mq}+\delta(q)f_{\mathrm{Ho}^{3+}})\times\exp[iq\psi+2\pi i(\mathbf{s}+q\boldsymbol{\tau})\cdot(\mathbf{r}_i+\mathbf{r}_j)], \tag{19}$$

where $\mathcal{E}$ is the amplitude scattered from a Thompson electron and $\boldsymbol{\kappa}$ is written as $2\pi\mathbf{s}$, where $|s|=2\lambda^{-1}\sin\theta$, λ being the x-ray wavelength and θ being half the scattering angle, not to be confused with the previous θ. Multiplying E by its complex conjugate yields the expression for the Laue-Bragg scattering

$$I_B=I_e\sum_{q=-6}^{q=6}|f_{Mq}+\delta(q)f_{\mathrm{Ho}^{3+}}|^2\times|\sum_{ij}\exp[2\pi i(\mathbf{s}+q\boldsymbol{\tau})\cdot(\mathbf{r}_i+\mathbf{r}_j)]|^2$$
$$\cong N_cI_eR^2\sum_{q=-6}^{q=6}|f_{Mq}+\delta(q)f_{\mathrm{Ho}^{3+}}|^2\times\delta((\mathbf{s}+q\boldsymbol{\tau})\cdot\mathbf{a}_1-H)\times\delta((\mathbf{s}+q\boldsymbol{\tau})\cdot\mathbf{a}_2-K)\times\delta((\mathbf{s}+q\boldsymbol{\tau})\cdot\mathbf{a}_3-L). \tag{20}$$

In Eq. (20), N_c is the number of unit cells in the crystal, I_e is the intensity scattered by a Thompson electron, $\mathbf{a}_1$, $\mathbf{a}_2$, and $\mathbf{a}_3$ are the vectors defining the unit cell, and the integers H, K, and L are the Miller indices. R is the geometrical structure factor defined as

$$R=\sum_i\exp[2\pi i(\mathbf{s}+q\boldsymbol{\tau})\cdot\mathbf{r}_i]. \tag{21}$$

From Eq. (20) we see that the Laue-Bragg maxima occur when

$$\mathbf{s}=H\mathbf{b}_1+K\mathbf{b}_2+L\mathbf{b}_3-q\boldsymbol{\tau}=\mathbf{B}_{HKL}-q\boldsymbol{\tau}, \tag{22}$$

where $\mathbf{b}_1$, $\mathbf{b}_2$, and $\mathbf{b}_3$ are the vectors reciprocal to $\mathbf{a}_1$, $\mathbf{a}_2$, and $\mathbf{a}_3$. The normal Laue-Bragg scattering is associated with $q=0$. In case none of the f_{Mq} is zero there are then satellite reflections at $\mathbf{B}_{HKL}\pm|q|\boldsymbol{\tau}$, with $q=1$, 2, 3, 4, 5, and 6, or six satellites in the direction of the spiral, in this case the $\mathbf{b}_3$ direction. When holmium is in the ferromagnetic state at $T<19.4$°K, examination of Table III shows that B_{pq} is nonvanishing for all q; *thus in the ferromagnetic state a maximum of six satellites can be expected.* In the antiferromagnetic state, 19.4°K $<T<131.4$°K, because of the flat spiral $\cos b\equiv 0$ and B_{pq} is nonvanishing only for even values of q. *In the antiferromagnetic state only three satellites can be expected.* Further, when $\boldsymbol{\kappa}$ and $\boldsymbol{\tau}$ are parallel, $\sin c\equiv 0$, and all B_{pq} vanish, except B_{p0}, and *no satellites will occur around the $(00\bar{0}\cdot L)$ reflections in either the ferromagnetic or antiferromagnetic state.* Figure 1 illustrates a portion of the reciprocal space of antiferromagnetic holmium in the vicinity of the $(22\bar{4}\cdot 0)$ reflection, solid circle, with the three satellite pairs the open circles, at the positions ± 2, ± 4, and $\pm 6\boldsymbol{\tau}$. If we assume the antiferromagnetic state but fill the $4f$ shell of the ions according to Hund's rule[19] then the $\Gamma_{43m_lm_s}{}^2(8)$'s in Table II are to be used in calculating the f_{8q}'s in Eq. (17). Assuming $\sin c=1$, and $\cos b=0$ the square of the scattering factor

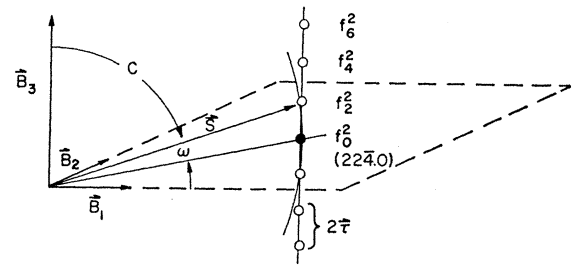

FIG. 1. Arrangement of satellites, open circles, about the $(22\bar{4}\cdot0)$ reflection, solid circle, in the holmium reciprocal lattice. The spacing between satellites is 2τ. The $\mathbf{B}_3$ axis lay in the plane of the diffractometer. The length of S was determined by the counter position, 2θ, and the crystal was step scanned through the angle ω.

of the first three satellite reflections, f_{82}^2, f_{84}^2, and f_{86}^2 are plotted as a function of $2\lambda^{-1}\sin\theta$ in Fig. 2. The position of the $(22\bar{4}\cdot0)$ reflection is indicated also. The intensity of the satellites is proportional to these f^2 values. *We note that the effects from the aspherical 4f shell are most pronounced not at small scattering angles but at intermediate angles.* The satellites are extremely weak compared to the normal Laue-Bragg reflections. At the $(22\bar{4}\cdot0)$ reflection where $f_{82}^2=1.96\times10^{-3}$, $f^2_{Ho^{3+}}=1.26\times10^3$, so even at this favorable position the ratio of the Laue-Bragg reflection to the first satellite pair is $\sim641\,000:1$. There is also an effect from the aspherical $4f$ shell on the intensity of the normal Laue-Bragg reflections through the factor f_{M0} in Eq. (20). However, f_{M0} is so small compared to $f_{Ho^{3+}}$ that experimental investigation of the effect is not feasible. It was on the basis of these results plotted in Fig. 2 that the choice of the $(22\bar{4}\cdot0)$ position and preliminary estimates of the satellite intensity were made.

The measured x-ray satellite intensities were found to be much less than those calculated from the f_{82}, which assumes that all ions are in the state $M=J$ on the basis of Hund's rule. This suggested that thermal disordering was inducing ionic states with $M<J$. Koehler *et al.*[8] observed a pronounced decrease in the

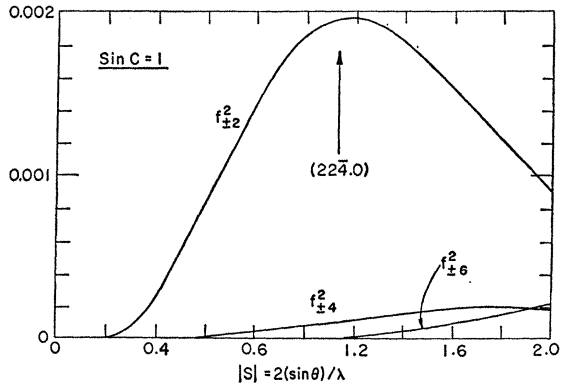

FIG. 2. The values of f_2^2, f_4^2, and f_6^2 versus $|S|=2\lambda^{-1}\sin\theta$ for the $4f$ shell filled according to Hund's rule with $\sin c=1$. Note that f_2^2 is approximately a maximum at the $(22\bar{4}\cdot0)$ reflection.

intensity of the neutron satellites in holmium as the temperature was raised. This can be understood if we write for p, the scalar part of the magnetic scattering amplitude[10]

$$p=(e^2\gamma/2mc^2)gJ\sigma f(\kappa), \tag{23}$$

where e^2/mc^2 is the scattering length of a Thompson electron, γ is the neutron moment in nuclear magnetons, $f(\kappa)$ is the magnetic form factor,[21] and σ is the fraction of the full moment J that is effective at a temperature T. At 77.5°K Koehler *et al.*[8] used a $\sigma=0.72\pm0.04$ for the effective moment. Thus the intensity of neutron satellites provides an excellent check on σ.

Nagamiya[12] has considered the effect of finite temperatures on screw structures of the type that we are considering with the approximation of the Weiss molecular field, and with this it is possible to calculate $\langle J\rangle=J\sigma$. The theory of screw structures assumes that within each plane of the structure the angular momenta of the ions are coupled ferromagnetically with an exchange constant V_0, between adjacent layers with an exchange constant V_1, and between nth layers with V_n, etc. The direction of quantization in any particular layer is the same, and twice the number of pairs interacting in the same way are included in the exchange constants. The energy is assumed equal to the dot product of the moments and the exchange constants. The angle between moments n layers apart is $n\pi\tau a_3$, where a_3 is the cell edge normal to the basal planes in holmium. The energy of the system is then

$$-\tfrac{1}{2}NJ^2V(\tau), \tag{24}$$

where

$$V(\tau)=\sum_n V_n\cos\pi n\tau a_3 \tag{25}$$

and N is the number of layers. The total energy is the sum on all spins; hence the factor $\frac{1}{2}$ in Eq. (24) so as not to count the same pair twice. A minimum in the energy corresponds to a maximum in $V(\tau)$. If $V(\tau)$ is a maximum for $\tau=0$ or a_3^{-1} the system will show ferromagnetism or antiferromagnetism, respectively. If neither of these is the case, the system will have a screw structure with a propagation vector τ which maximizes $V(\tau)$. In Eq. (24) J is normally the maximum component of angular momentum along the direction of quantization. The effect of a finite temperature is included by replacing J by the thermal average $\langle J\rangle=J\sigma$. The so-called Weiss field consistent with this energy[22] is $-(g\mu_B)^{-1}J\sigma V(\tau)$. A single ion with the component M of angular momentum in the direction of quantization will interact with the Weiss field with an energy $-MJ\sigma V(\tau)$. The probability that such an ion will have the component M is given by the appropriate Boltzmann factor, and the expectation value for $M,J\sigma$, will

[21] See, e.g., Ref. 12; in M. Blume, Phys. Rev. 130, 1670 (1963).
[22] See, e.g., R. Brout, in *Magnetism*, edited by G. T. Rado and H. Suhl (Academic Press Inc., New York, 1965), Vol. IIA, p. 43.

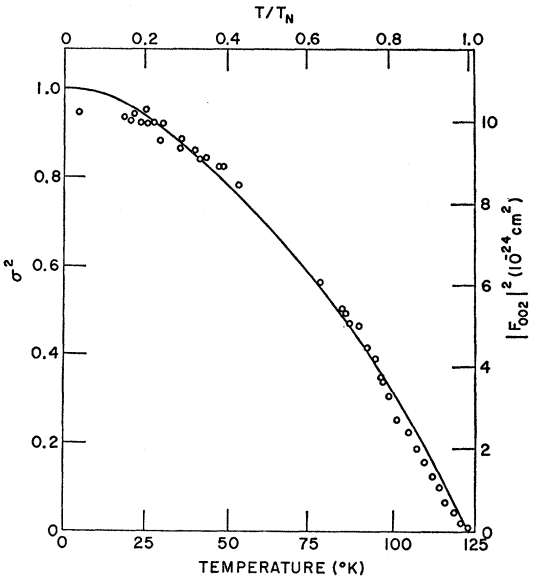

FIG. 3. The square of σ, the fraction of J effective at the temperature T versus T. The Brillouin dependence of σ is found by solving for self-consistency, Eq. (28). The ordinates on the left are for σ^2 and those on the right are for $|F_{002}|^2$, the structure factor for the neutron satellite pair about $(00\bar{0}.2)$. The points are the measurements of Koehler *et al.*

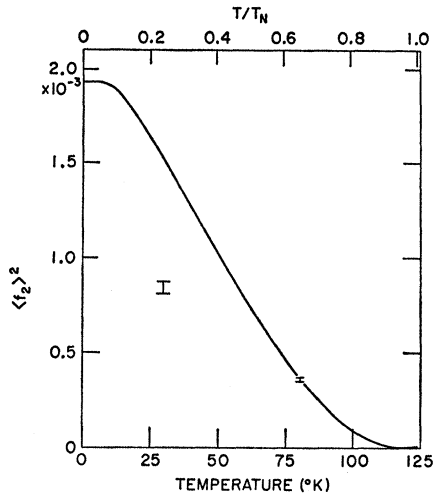

FIG. 4. Plot of $\langle f_2\rangle^2$ for the first x-ray satellite pair about the $(22\bar{4}\cdot 0)$ reflection versus temperature using the f_{M2}'s of Table IV weighted according to Eq. (29). The decrease with temperature is much more rapid than the neutron case of Fig. 3. The two points shown are the experimental x-ray values.

be found from the equation of self-consistency,

$$J\sigma=\sum_{M=-J}^{M=J} Me^{MJ\sigma V(\tau)/kT}\Big/\sum_{M=-J}^{M=J} e^{MJ\sigma V(\tau)/kT}$$
$$=JB(J^2\sigma V(\tau)/kT), \quad (26)$$

where $B(J^2\sigma V(\tau)/kT)$ is the Brillouin function. When σ becomes vanishingly small at the Néel temperature T_N, Eq. (26) requires that

$$T_N=J(J+1)V(\tau)/3k. \quad (27)$$

Substituting for $V(\tau)$ in terms of the Néel temperature in Eq. (26) we can write

$$\sigma=B(3J\sigma T_N/(J+1)T). \quad (28)$$

In Fig. 3 we have plotted σ^2 as a function of temperature along with the measurements of the structure factor for the $(00\bar{0}\cdot 2)$ satellite of Koehler *et al.*[8] In the figure, values on the left ordinate are for σ^2 and on the right for $|F_{002}|^2$. The agreement above $\sim 20°$K is excellent. The lack of agreement below 20°K can be ascribed to the ferromagnetic transition at 19.4°K. This agreement with the neutron results were so encouraging that the average x-ray scattering factor was evaluated from

$$f_q=\sum_{M=-J}^{M=J} f_{Mq}e^{3M\sigma T_N/(J+1)T}\Big/\sum_{M=-J}^{M=J} e^{3M\sigma T_N/(J+1)T}$$
$$=\frac{\sinh[3\sigma T_N/2(J+1)T]}{\sinh[3(2J+1)\sigma T_N/2(J+1)T]}$$
$$\times\sum_{M=-J}^{M=J} f_{Mq}e^{3M\sigma T_N/(J+1)T}. \quad (29)$$

Figure 4 is a plot of $\langle f_2\rangle^2$ for the first satellite pair about the $(22\bar{4}\cdot 0)$ reflection versus temperature. The f_{M2}'s of Eq. (17) were calculated using the values $\langle j_2(\kappa)\rangle_{4f}=0.196$, $\langle j_4(\kappa)\rangle_{4f}=0.0505$, and $\langle j_6(\kappa)\rangle_{4f}=0.0110$ interpolated from the values given by Blume *et al.*[13] For evaluating the coefficients B_{p2} of Table III the angles b and c were taken to be 90.0° and 86.53°, respectively. The values of f_{M2} for the first satellite pair about the $(22\bar{4}\cdot 0)$ reflection for the holmium ion in the state with inner quantum number $J=8$ and magnetic quantum numbers M are listed in Table IV. These f_{M2}'s were then weighted according to Eq. (29) to determine $\langle f_2\rangle$. The decrease of $\langle f_2\rangle^2$ with temperature is much more pronounced than for the neutron case and is due to the almost quadratic dependence of the f_{M2} upon M in contrast to the linear dependence of the neutron scat-

TABLE IV. Values of f_{M2} from Eq. (17) for the first satellite pair about the $(22\bar{4}\cdot 0)$ reflection for the holmium ion in the state with inner quantum number $J=8$ and magnetic quantum numbers M.

$\lvert M\rvert$	8	7	6	5	4	3	2	1	0
f_{M2}	+0.0439	+0.0298	+0.0183	+0.00679	−0.00516	−0.0167	−0.0264	−0.0329	−0.0352

tering amplitude on M. The two points in the figure are the experimental values and their determination is discussed in the next section.

The treatment leading to Eqs. (28) and (29) implicitly assumed that $V(\tau)$ is independent of the temperature or σ, and has the value determined by the Néel temperature in Eq. (27). Experimentally[7] the turn angle varies over the range $30°\leq\pi\tau a_3\leq 51°$ between the Curie and Néel temperatures. However, $V(\tau)$ will remain very nearly stationary if either V_0 is the dominant interaction energy in Eq. (25) or if $V_2/V_1=-0.62055$, $V_3/V_1=+0.26790$, $V_4/V_1=-0.07307$, and $V_5/V_1=+0.00970$.

EXPERIMENT

A single crystal of holmium was obtained on loan from the Ames Laboratory. The crystal had been grown in the solid phase by the strain-anneal method. Impurities were Ca$<$500 ppm, Fe$\leq$20 ppm, Ta$\leq$500 ppm, Si$\leq$50 ppm, C$\leq$60 ppm, Mg$\leq$10 ppm, Cr$<$50 ppm, Ni$\leq$50 ppm, O=335 ppm, H=32 ppm, and N=24 ppm. (ppm is parts per million by weight.) The crystal was faced upon $(11\bar{2}\cdot 0)$ and after suitable metallographic polishing and etching the crystal proved to be free of inclusions and parasite crystals. Back-reflection Laue photographs were of excellent quality and orientation. The position of the neutron satellites at 77.4°K reported by Koehler[7] were confirmed for this crystal by measuring the positions of the $(11\bar{2}\cdot 0)$ and $(22\bar{4}\cdot 0)$ neutron satellite pairs from the crystal.

The crystal was mounted inside a modified Materials Research Corporation model X-86 GC cryostat with the $(11\bar{2}\cdot 0)$ face aligned on the vertical ω axis of the Picker diffractometer. The hexagonal axis was aligned normal to the ω axis or in the horizontal plane of the diffractometer. Monochromatized Cu $K\alpha$ radiation was obtained from a doubly bent LiF crystal after Schwartz *et al.*[23] with $TM=MF=11.43$ cm, $FF''=34.00$ cm. Curved tantalum slits were inserted between T and M and at F, such that AM was the generatrix of the area illuminated on the LiF crystal. The monochromator eliminated fluorescence problems with the possible exception of that from the holmium L_{III} level at 1.5368 Å which could be excited by the radiation passed by the monochromator window along with Cu $K\alpha_1$ (1.5406 Å) and Cu $K\alpha_2$ (1.5444 Å). The Dunlee DZ-1BH high intensity tube was normally operated at 40-kV constant potential and 26 mA. The most intense beam was found at 2° take-off angle for which the projected focal spot was 0.52 mm wide and 1.50 mm high. This large focal spot size and abberations in the LiF monochromator prevented good vertical focusing and when the vertical height of the beam was set at 6 mm at F, the horizontal focus, the beam at F'', the counter slit, was still about 5 mm high. This geometry was chosen to that the approximate line focus at F was symmetrically refocused at F'' by any $(HH\overline{2H}\cdot 0)$ reflection of the holmium crystal. In order to investigate a satellite reflection, the crystal had to be turned out of this symmetrical focusing condition through the angle ω as in Fig. 1. However, asymmetrical focusing[24] could be achieved keeping FF'' constant by making the ratio $FF'/F'F''=\sin(\theta-\omega)/\sin(\theta+\omega)$. The diffractometer was mounted upon a milling machine which allowed such changes to be made accurately. Intensities taken in the asymmetrical condition were corrected to the symmetrical condition[25] by multiplying by $1-\tan\omega/\tan\theta$. Since the satellite reflections were expected to be as sharp as the normal Laue-Bragg reflections, but extremely weak, it was imperative that the peak to background be kept at a maximum consistent with an over-all high counting rate. This meant that the volume element defined by the various divergences should be comparable to the dimensions of the Laue-Bragg reflections from the holmium crystal including its mosaic spread. To this end experiments were carried out at room temperature to maximize the Laue-Bragg peak to the background in the vicinity of the satellites. The final slit arrangements chosen were: incident focal slit F, 0.50 mm wide by 6.0 mm high with a 0.16° horizontal divergence, receiver slit F'' 0.48 mm wide by 10.0 mm high followed by a 4° antiscatter slit and 2° vertical soller slits. The monochromatized beam was monitored after passing through slit F and the air path length to both monitor and counter detectors was the same. Scintillation detectors with pulse-height selection were used on both channels. Hamner solid-state electronics and semi-automated control of ω or 2θ axis were employed.

Scans at 77.4°K through the $(22\bar{4}\cdot 0)$, $(22\bar{4}\cdot\bar{2})$, and $(22\bar{4}\cdot 2)$ reflections confirmed the lattice constants reported by Darnell.[26] Using the values of τ determined by Koehler *et al.*,[7] a search program was carried out in the vicinity of both the $(11\bar{2}\cdot 0)$ and $(22\bar{4}\cdot 0)$ reflections for the first satellite pairs. The diffractometer was programmed to step scan ω through an arc which included the first satellite pair for various settings of $|s|$ (see Fig. 1). The values of $|s|$ were determined by the counter position 2θ. Figure 5 is the average of 10 ω scans through the first satellite pair about the $(22\bar{4}\cdot 0)$ reflection at 77.4°K (liquid N_2) after the optimum counter position for the Cu $K\alpha_1$ component was found. The background of 8200 counts represents a counting rate of ~4.8 counts/sec. The satellites at $(11\bar{2}\cdot 0)$ were also detected but the peak to background was much inferior to that at $(22\bar{4}\cdot 0)$. From the lattice constants[26]

[23] L. H. Schwartz, L. A. Morrison, and J. B. Cohen, in *Advances in X-Ray Analaysis*, edited by W. M. Mueller, G. Mallet, and M. Fay (Plenum Press, Inc., New York, 1964), Vol. 7, p. 281.

[24] A. Guinier, *X-Ray Crystallographic Technology* (Adam Hilger Ltd., London, 1952), p. 101.

[25] R. J. Weiss, in *X-Ray Determination of Electron Distributions*, edited by E. P. Wohlfarth (John Wiley & Sons, Inc., New York, 1966), Vol. VI, p. 109.

[26] F. J. Darnell, Phys. Rev. **130**, 1825 (1963).

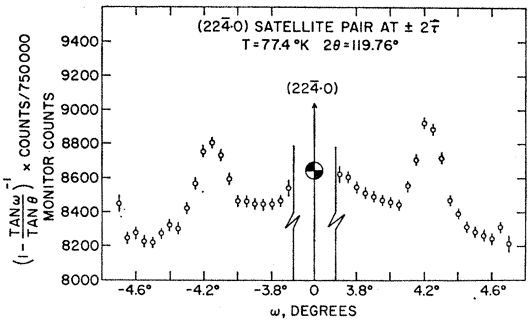

FIG. 5. The average of ten scans through the first satellite pair about the (22$\bar{4}$·0) reflection at 77.4°K (liquid N_2) for the optimum counter position of the Cu $K\alpha_1$ component.

and neutron value[7] of τ the position of the same satellite pair at 27.3°K (liquid neon) for the Cu $K\alpha_1$ component was computed. Figure 6 is the average of ten ω scans at 27.3°K. The satellites are closer to the (22$\bar{4}$·0) reflection in agreement with the neutron results. The intensity of the satellites is much larger than at 77.4°K. The background is approximately 7% less than at 77.4°K and this is ascribed to a reduction in the thermally scattered x rays in the neighborhood of the (22$\bar{4}$·0) reflection.

The integrated reflection from a crystal is a pure number given by[27]

$$\frac{E\dot{\omega}}{P_0}=\int R(\omega)d(\omega), \tag{30}$$

where $R(\omega)$ is the fraction of the incident power P_0 reflected at the angle ω, and E is the total energy reflected when the scan rate is $\dot{\omega}$. In Eq. (30) the counter slits are assumed to be large enough so that any fraction of the incident power reflected by the crystal is detected. However, because of the unfavorable peak to background for the satellites, the horizontal width of the counter slits had to be kept too small to satisfy this condition. Nevertheless, by incrementing the

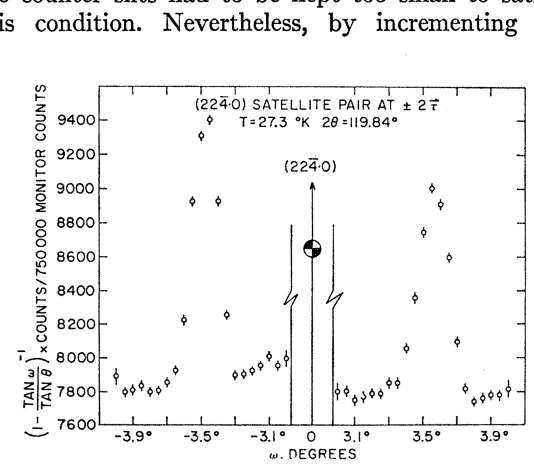

FIG. 6. Same as for Fig. 5 but at 27.3°K (liquid neon).

[27] See Ref. 14, p. 45.

counter by amounts $\Delta 2\theta$ corresponding to the angle subtended by the receiver slit at F'', repeating the ω scans and adding them together, the condition of a large counter slit could be fulfilled. Actually, advantage was taken of the close proximity of the satellites to the (22$\bar{4}$·0) reflection to employ the following scheme. At reduced power levels, 16 kV and 4 mA, the optimum counter position for the Cu $K\alpha_1$ component for the (22$\bar{4}$·0) reflection was found, and an ω scan with the counter at this position similar to those through the satellites in Figs. 5 and 6 was made. The counter was then incremented in steps of $\Delta 2\theta$ on both sides of this optimum setting and the ω scans added together to obtain the integrated reflection. It was found that the integrated reflection was 2.44 times larger than the ω scan made at the optimum counter setting for the Cu $K\alpha_1$ component. The optimum scan through the satellites was then multiplied by this factor to determine their integrated reflection.

The main beam power was measured by scanning the counter, with the same slit arrangement, through the beam with the cryostat slightly displaced so that the beam missed the crystal but was still attenuated by the windows and radiation shields. This measurement was made with five nickel foils in the beam that reduced it by a factor of 52.2. The main beam power was then calculated to be 1.97×10^5 counts per monitor count. The reflected power of 6.62 counts per monitor count for the (22$\bar{4}$·0) reflection gives an integrated reflection of 3.37×10^{-5}. The integrated reflection for an ideally imperfect crystal in reflection geometry is

$$\frac{E\dot{\omega}}{P_0}=\left(\frac{e^2}{mc^2}\right)^2\frac{N_c^2\lambda^3}{2\mu\sin2\theta}\left(\frac{1+\cos^2 2\theta_m\cos^2 2\theta}{1+\cos^2 2\theta_m}\right)\times R^2|f|^2e^{-2B[(\sin\theta)/\lambda]^2}$$

$$=1.14\times10^{-7}|f|^2e^{-2B[(\sin\theta)/\lambda]^2}, \tag{31}$$

for the (22$\bar{4}$·0) reflection, where the Thompson cross section $(e^2/mc^2)^2=7.94\times10^{-26}$ cm^2, the number of unit cells per unit volume $N_c=1.60\times10^{22}$ cm^{-3}, the x-ray wavelength $\lambda=1.54\times10^{-8}$ cm, the linear absorption coefficient[28] $\mu_l=1.12\times10^3$ cm^{-1}, the monochromator scattering angle $2\theta_m=45.022°$, the crystal scattering angle is 2θ, and the geometrical structure factor for the (22$\bar{4}$·0) reflection $R=2$, f is the atomic scattering factor, and B is the Debye parameter. Equation (31) was used to compute the integrated (22$\bar{4}$·0) reflection at 77.4°K. For this temperature a value of $B=0.275\times10^{-16}$ cm^2 was interpolated from those values tabulated for gadolinium.[28] The value of f was computed from

$$f=f_{\text{Ho}^{3+}}+\Delta f'+i\Delta f'', \tag{32}$$

[28] *International Tables for X-Ray Crystallography*, edited by C. H. MacGillavry, G. D. Rieck, and K. Lonsdale (Kynock Press, Birmingham, 1962), Vol. III, Sec. 3.

where $f_{Ho^{3+}}=35.5$ was interpolated from the values of Blume *et al.*,[13] $\Delta f'$ the real part of the dispersion correction is listed variously as -13.0 [28] or -10.5 [29] and the imaginary part of the dispersion correction $\Delta f''=3.0$.[28] Depending on the value assumed for $\Delta f'$ the integrated $(22\bar{4}\cdot 0)$ reflection calculated from Eq. (31) is either 4.92×10^{-5} or 6.06×10^{-5}. The fact that the observed integrated reflection was less than this is attributed to primary extinction.[30,31] If the holmium crystal had ideally perfect regions of approximately 3–5 μ thickness, the discrepancy between the measured and computed value is satisfactorily explained.[30]

Fortunately, the satellite reflections are so weak that the crystal could be considered as ideally imperfect and free of extinction. The dispersion corrections to the f_{Mq}'s in Eq. (17) are negligible since the incident radiation frequency was 2000 times larger than the N_{VI} and N_{VII} absorption edges associated with the $4f$ electrons.[32] The reflected powers of the two satellites at 77.4°K when multiplied by the factor 2.44 were 6.95×10^{-6} and 6.73×10^{-6} counts per monitor count for the positive and negative satellite, respectively. The corresponding reflected powers of the two satellites at 27.3°K were 16.7×10^{-6} and 17.8×10^{-6} counts per monitor count, respectively. The corresponding integrated reflections at 77.4°K are 3.52×10^{-11} and 3.42×10^{-11}. Using the Debye parameter $B=0.275\times10^{-16}$ cm^2, these values correspond to values of $\langle f_2\rangle=0.0192$ and 0.0189, respectively. The theoretical value using the f_{Mq}'s of Table IV weighted according to Eq. (29) is 0.020. The corresponding integrated reflections at 27.3°K are 8.50×10^{-11} and 9.04×10^{-11}. Using the Debye parameter[28] $B=0.145\times10^{-16}$ cm^2 these values correspond to values of $\langle f_2\rangle=0.0286$ and 0.0295, respectively. The theoretical value is 0.0398. The values of $\langle f_2\rangle^2$ corresponding to these values are also shown in Fig. 4. It should be mentioned, perhaps, that the theoretical curve of Fig. 4 assumes that the angle c remains constant at 86.53° while in fact this angle changes slightly with temperature because of the change in τ with temperature.[7]

[29] L. R. Saravia and S. Catichaellis, Acta Cryst. **20**, 927 (1966).
[30] See Ref. 14, Chap. 6.
[31] See Ref. 25, Vol. VI, p. 44.
[32] In order to estimate the possible effect, assume that the $4f$ electrons' contribution to the atomic absorption coefficient varies inversely as the cube of the frequency of the incident radiation frequency ω, and that ω_N is the N absorption edge for the $4f$ electron. Then if the oscillator strength of the $4f$ electrons is taken as unity, $\Delta f'\approx(\omega_N/\omega)^2\ln|(\omega_N/\omega)^2-1|$ and $\Delta f''\approx\pi(\omega_N/\omega)^2$ or 4.0×10^{-6} and 0.7×10^{-6}, respectively; see Ref. 14, p. 149. These small corrections are, of course, applicable to the $\langle j_0(\kappa)\rangle_{4f}$ and not to the aspherical terms. However, it seems reasonable that the corrections to the f_{Mq}'s are of similar magnitude.

CONCLUSIONS

The scattering of x rays as a function of both the magnitude and direction of $\boldsymbol{\kappa}$ by the nonspherical $4f$ charge density in the holmium ion characterized by the inner quantum number $J=8$ and magnetic quantum number M was derived. It was then shown that when the direction of quantization $\mathbf{z}$ of the ions is that of a flat spiral so that the angle between $\mathbf{z}$ and $\boldsymbol{\kappa}$ varies periodically, that three x-ray satellite reflections appear with spacings in multiples of $\pm2\tau$, where τ is the propagation of vector of the spiral. However, in order to achieve agreement with experiment it was necessary to assume that at a finite temperature the ions are disordered to the extent that they are distributed amongst the various states M. The nature of this distribution was determined using the molecular-field approximation. This theory of the disorder explains quite well past observations of the change in neutron satellite intensities with temperature. These results were so encouraging that the theory was used to compute the average x-ray scattering factor $\langle f_2\rangle$ from the scattering factors f_{M2} of the various states M whose computation rest upon parameters derived from recently determined Hartree-Fock rare-earth wave functions. The agreement with experimentally observed values of $\langle f_2\rangle$ for the first x-ray satellite pair about the $(22\bar{4}\cdot 0)$ reflection discussed in the paper is good.

Note added in manuscript. A recent communication by Jennings[33] sites a possible error in using the polarization factor in Eq. (31). Using Jenning's experimental value of $k_e=0.772$ in place of $\cos2\theta_m=\cos45.002°$ and assuming no extinction in the satellite reflections reduces the polarization factor of Eq. (31) by $\sim8\%$.

ACKNOWLEDGMENTS

The author is deeply indebted to Dr. M. Blume for suggesting this challenging and stimulating problem and to Professor F. H. Spedding whose loan of an excellent holmium single crystal made this research possible. He wishes also to thank Dr. W. C. Koehler for permission to reproduce the neutron measurements in Fig. 4 and for his discussions pertinent to those measurements. He is indebted to Dr. G. Shirane for his measurements confirming the positions of the neutron satellites from the crystal used in the x-ray experiment. The author also wishes to thank Dr. R. Watson and Dr. M. Blume for their help and discussions bearing on the various properties of the rare earths. Finally, he wishes to thank Miss Estarose Wolfson who programmed on the CDC 6600 the tedious operations leading to the values in Table II.

[33] L. D. Jennings, Acta Cryst. A24, 472 (1968).